Screening Membrane Interactions of Pesticides by Cells Decorated with Chromatic Polymer Nanopatches

ARTICLE *in* CHEMICAL RESEARCH IN TOXICOLOGY · JANUARY 2009

Impact Factor: 3.53 · DOI: 10.1021/tx800206t · Source: PubMed

5 AUTHORS, INCLUDING:

Agnieszka Mech-Dorosz
Technical University of Denmark
3 PUBLICATIONS **15** CITATIONS
SEE PROFILE

Zulfiya Orynbayeva
Drexel University College of Medicine
27 PUBLICATIONS **380** CITATIONS
SEE PROFILE

Sofiya Kolusheva
Ben-Gurion University of the Negev
78 PUBLICATIONS **2,259** CITATIONS
SEE PROFILE

Chemical Research in Toxicology

Article

Screening Membrane Interactions of Pesticides by Cells Decorated with Chromatic Polymer Nanopatches

Agnieszka Mech, Zulfiya Orynbayeva, Kaiyr Irgebayev, Sofiya Kolusheva, and Raz Jelinek

Chem. Res. Toxicol., **2009**, 22 (1), 90-96• DOI: 10.1021/tx800206t • Publication Date (Web): 31 December 2008

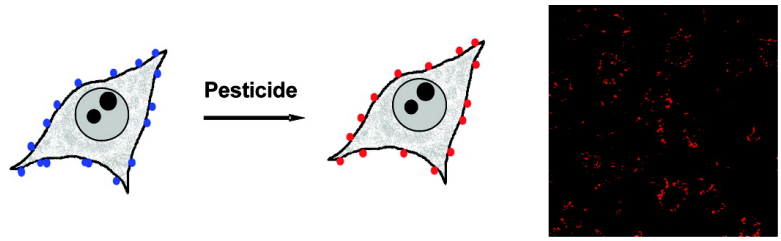

More About This Article

Additional resources and features associated with this article are available within the HTML version:

- Supporting Information
- Access to high resolution figures
- Links to articles and content related to this article
- Copyright permission to reproduce figures and/or text from this article

View the Full Text HTML

Chemical Research in Toxicology is published by the American Chemical Society.
1155 Sixteenth Street N.W., Washington, DC 20036

Screening Membrane Interactions of Pesticides by Cells Decorated with Chromatic Polymer Nanopatches

Agnieszka Mech, Zulfiya Orynbayeva,† Kaiyr Irgebayev, Sofiya Kolusheva, and Raz Jelinek*

Ilse Katz Institute for Nanotechnology and Department of Chemistry, Ben Gurion University of the Negev, Beer Sheva 84105, Israel

Received June 8, 2008

Elucidating the factors contributing to the cell toxicity of pesticides and other environmentally sensitive small molecules is critical for evaluation of their health impacts and for understanding the biological processes that they affect. Disruption and permeation of the plasma membrane, which constitutes the critical interface between the cell and its environment, are recognized initiators of cytotoxicity. We present a new approach for predicting pesticide cytotoxicity through rapid screening of membrane interactions of pesticides using a recently developed live-cell chromatic sensor. The sensing platform comprises living mammalian cells labeled with polydiacetylene (PDA), a chromatic polymer that undergoes intense fluorescence transformations induced by structural perturbations of the membrane bilayer. Within a short time after the addition of membrane-interacting tested compounds to the labeled cells, the PDA patches emit high fluorescence, which can be monitored by conventional spectroscopy and microscopy apparatuses. The chromatic technology facilitates rapid evaluation of membrane activity of pesticide compounds and is capable of distinguishing between toxic effects associated with membrane interactions vs intracellular mechanisms.

Introduction

Toxicology analysis of pesticides almost exclusively focuses upon their effects on downstream cellular processes and phenomena such as alterations of neuroreceptors, sodium channel functionalities, modifications of cell energetic states, apoptotic effects, and others (*1, 2*). The plasma membrane, however, is the primary physiological barrier and essentially the first cell constituent encountered by biologically active molecules. Furthermore, shifts in the molecular properties of boundary lipids might have pronounced cellular consequences, leading to changes in ion channel conformations or interfering with bilayer-embedded receptor proteins. Several studies have analyzed interactions of pesticides with lipid bilayers (*3*−*6*). Pyrethroids, for example, modulate membrane packing order by destabilizing lipid fluid phase (*7*). Varied pesticide compounds were shown to induce perturbations in both the hydrocarbon chain and the polar head regions of lipid vesicles (*8, 9*). However, utilization of membrane interactions as a practical screening and predictive tool for toxic effects has been rare.

Here, we demonstrate a new approach for evaluation and rapid screening of pesticide interactions with the plasma membrane through application of a recently developed living-cell membrane sensor (*10*−*12*). The experimental platform comprises live mammalian cells in which the plasma membrane has been decorated with polydiacetylene (PDA) nanopatches (*11*). PDA is a conjugated polymer that undergoes rapid colorimetric (blue−red) and fluorescence transformations (*13*), which are induced by external structural perturbations (*11, 14*). The chromatic properties of PDA have been exploited in recent years for diverse biosensing applications, utilizing different PDA-based assemblies, including small vesicles (*15*), giant vesicles (*16*), semisolid porous matrixes (*17*), films (*18*), and others. PDA-labeled cells, in particular, recently developed in our laboratory, facilitate spectroscopic and microscopic analysis of molecular events occurring in the actual environment of the plasma membrane in a living cell (*10*−*12*).

The thrust of this work is the close relationship between membrane bilayer perturbation and cytotoxicity, observed in varied physiological phenomena (*19*). We show that membrane disruption events can be easily detected using PDA-labeled monolayer cells. The analysis is significantly much faster than conventional toxicology screening, pointing to the potential use of PDA-labeled cells as cytotoxicity predictors.

Experimental Procedures

Materials. Lipids, including 1,2-dimyristoyl-*sn*-glycero-3-phosphoethanolamine (DMPE) and 1,2-dimyristoyl-*sn*-glycero-3-[phospho-rac-(1-glycerol)] (DMPG), were purchased from Avanti Polar Lipids, Inc. (Alabaster, AL). The diacetylenic monomer 10,12-tricosadiynoic acid was purchased from Alfa Aesar (Karlsruhe, Germany).

1-(4-Trimethylammoniumphenyl)-6-phenyl-1,3,5-hexatriene (TMA-DPH) was obtained from Molecular Probes, Inc. (Eugene, OR). The MTS proliferation assay was purchased from Promega Corp. (Madison, WI). The pesticide compounds diazinon, chlorperifos, paraoxon-methyl, allethrin, cypermethrin, permethrin, barban, carbaryl, carboxin, linuron, diuron, pronamide, isoxaben, and iprodion were purchased from Sigma-Aldrich. The chemical purity of 95.3−99% was reported for all compounds.

Preparation of Pesticide Solutions. Stock solutions of concentrated compounds in DMSO were prepared, followed by dilution in HEPES buffer (20 mM HEPES, 137 mM NaCl, 2.7 mM KCl, 1 mM KH_2PO_4, and 5 mM D-glucose, pH 7.4) to 100 μM prior to addition to the cells.

* To whom correspondence should be addressed. E-mail: razj@bgu.ac.il.
† Current address: Department of Biochemistry and Molecular Biology, Drexel University College of Medicine, Philadelphia, Pennsylvania 19129.

10.1021/tx800206t CCC: $40.75
Published on Web 12/31/2008

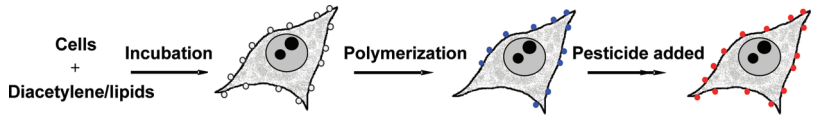

Figure 1. Experimental scheme of screening pesticide/membrane interactions with PDA-labeled cells. Cells were incubated with diacetylene/lipid vesicles followed by polymerization by UV irradiation. Bilayer interactions after the addition of membrane-active compounds give rise to the blue−red (and fluorescence) transformations of the surface-attached PDA nanopatches.

Cell Culture. Human epidermoid carcinoma cells A431 were grown in DMEM medium supplemented with 10% (v/v) heat-inactivated fetal calf serum, 4 mM L-glutamine, 50 U/mL penicillin, and 50 μg/mL streptomycin in a humidified 5% CO_2 atmosphere at 37 °C.

Vesicle Preparation. 10,12-Tricosadiynoic acid (the diacetylene monomer) was washed in chloroform and passed through a 0.45 μm nylon filter prior to use. The vesicle constituents 10,12-tricosadiynoic acid, DMPE, and DMPG were dissolved in a chloroform/ethanol solution (1:1) at a molar ratio of 3:1:1 and dried in vacuo up to constant weight. The dry monomer/lipid film was subsequently probe-sonicated in deionized water at 70 °C for 4 min and for another 4 min without heating. The vesicle solution was then cooled and kept at 4 °C overnight. The total lipid concentration of the diacetylene/DMPE/DMPG vesicle solution was 7.3 mM.

PDA-Labeled Cells and Fluorescence Spectroscopy. Cells were seeded on 24 well plates to full confluence the day before the experiment and subsequently washed with HEPES buffer. The diacetylene/DMPE/DMPG vesicles (final lipid concentration of 0.4 mM) were added to the cells in HEPES buffer in a 1.5 mL volume and incubated for 30 min with strong shaking. Following incubation, the labeled cells were irradiated for 30 s at 254 nm using a hand-held UV lamp (UVC-16, Ultra Lum Inc. Claremont, Canada) or a BLX-254 UV-Cross-linker (Marne La Vallee, France) to achieve polymerization of PDA. Irradiation resulted in an intense blue appearance of the cell monolayer. The unbound vesicles were subsequently removed through careful washing several times, and fresh HEPES buffer was added before conducting measurements. All experimental steps were carried out at 25 °C. Cell viability after treatment was more than 90% as determined by the Trypan blue exclusion assay.

Pesticide compounds were applied in all experiments at high (toxic) concentrations of 500 μM (nominal concentrations; for actual concentrations, see Table 1 of the Supporting Information); the final DMSO concentration was 0.2%. Steady-state emission spectra of the plates were acquired at 25 °C on a Fluoscan Ascent spectrofluorimeter (Vantaa, Finland) using 485 nm excitation and emission at 555 nm. The net fluorescence intensities (accounting for the control fluorescence from the same volume without pesticide present) were reported as percentages as compared to the maximal PDA fluorescence, obtained by heating the lipid/PDA vesicles to produce the highly fluorescent red PDA phase. All experiments were repeated at least three times.

Fluorescence Anisotropy. The fluorescence probe TMA-DPH was incorporated into the cell membrane by adding the dye dissolved in THF (1 mM) to a cell suspension in HEPES buffer up to a final concentration of 1.25 μM (solvent final concentration 0.1%). After 30 min of incubation at 37 °C with gentle stirring, the cells were washed three times with HEPES buffer for removal of excess fluorescent probe. DPH fluorescence anisotropy was measured at 428 nm (excitation 360 nm) on an FL920 spectrofluorimeter (Edinburgh Co., Edinburgh, United Kingdom). Anisotropy values (r) were automatically calculated by the spectrofluorimeter software. Fluorescence anisotropy measurements were performed four times.

Fluorescence Microscopy. Cell samples for microscopy analysis were prepared according to the procedure described above (Fluorescence Anisotropy), except that cells were seeded on 35 mm glass-bottom MatTek dishes. Fluorescence images of the PDA-labeled cells were acquired on a laser-scanning confocal microscope Axiovert-100 M (Zeiss, Germany) with a Plan-Neofluar 63×/1.2 oil objective. The excitation wavelength at 488 nm was produced by an argon laser. Emitted light was passed through a LP 505nm filter.

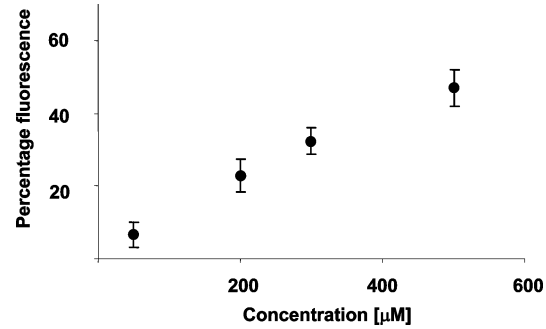

Figure 2. Chromatic dose−response curve for diazinon. The induced fluorescence due to membrane interactions of diazinon with PDA-labeled cells is presented as a percentage of the maximal fluorescence of the PDA-labeled cells. The concentration values indicated are the nominal concentrations.

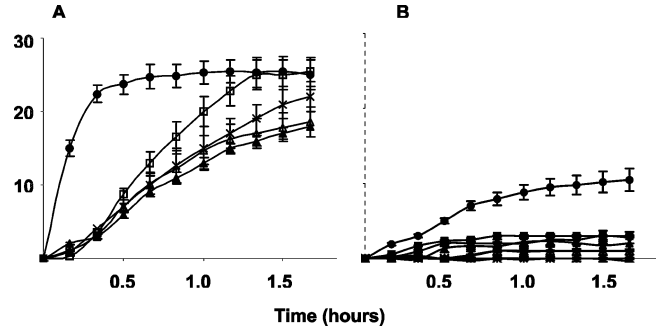

Figure 3. Fluorescence emission of PDA-labeled A431 cells incubated with pesticides. The induced fluorescence due to membrane interactions of the pesticide compounds is presented as a percentage of the maximal fluorescence of the PDA-labeled cells. All compounds were added at 100 μM. Symbol key: (A) ×, diuron; □, barban; △, diazinon; ▲, allethrin; and ●, chlorperifos. (B) □, carbaryl; △, linuron; ◊, cypermethrin; ▲, carboxin; ◆, paraoxon; ■, permethrin; ▲, pronamide; ×, iprodion; and +, isoxabene.

Cell Proliferation. The cytotoxicity of the pesticides was assessed using a cell proliferation assay (Promega CellTiter 96 AQueous One) (*20*). Briefly, exponentially growing cells were seeded in 96 well microculture plates in 100 μL volumes. Immediately and after 24 h of incubation at 37 °C, 20 μL aliquots of 3-(4,5-dimethylthiazol-2-yl)-5-(3-carboxymethoxyphenyl)-2-(4-sulfophenyl)-2H-tetrazolium, inner salt (MTS), were added to each well, and the samples were incubated for another 1.5 h at 37 °C. Plates were analyzed on FLASHScan S12 Micro plate Reader (Jena Analytical, Jena, Germany) at 490 nm. For each compound, three replicates were recorded in each of the three days of experiments.

Results and Discussion

Figure 1 depicts the experimental scheme. Cells were incubated with the diacetylene/phospholipid vesicles followed by irradiation at 254 nm to achieve membrane labeling with the chromatic PDA patches. A431 cells were used in the experiments discussed here to best mimic the environment of the skin barrier; however, the technology can be easily

Table 1. Tested Molecules, Structures, Families, and Toxicological Effects (References)

Compound name	Chemical structure	Compound family	References
Diazinon	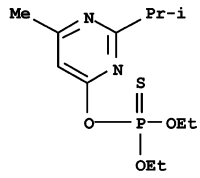	**Organophosphates**	(*21-23*)
Chlorperifos	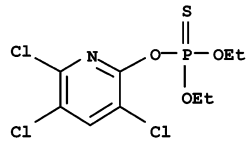	**Organophosphates**	(*24, 25*)
Paraoxon	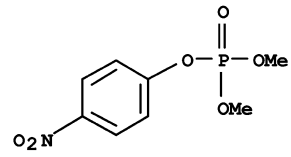	**Organophosphates**	(*25, 26*)
Allethrin	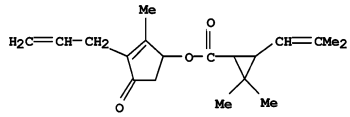	**Pyrethroids**	(*27-29*)
Cypermethrin	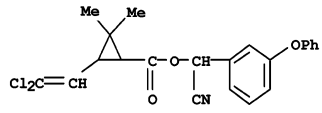	**Pyrethroids**	(*23, 30*)
Permethrin	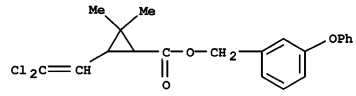	**Pyrethroids**	(*31, 32*)
Barban	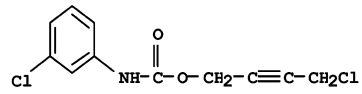	**Carbamates**	(*33, 34*)
Carbaryl	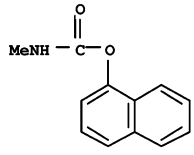	**Carbamates**	(*35, 36*)
Carboxin	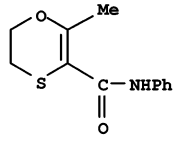	**Carbamates**	(*37, 38*)
Linuron	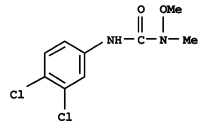	**Organochlorines**	(*39, 40*)

Table 1. Continued

Compound name	Chemical structure	Compound family	References
Diuron	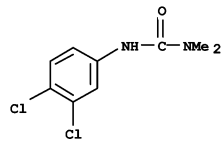	**Organochlorines**	(*41, 42*)
Pronamide	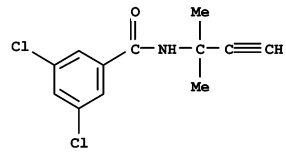	**Amides**	(*43*)
Isoxaben	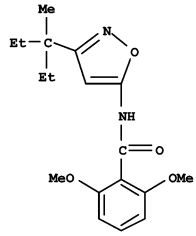	**Amides**	(*42*)
Iprodion	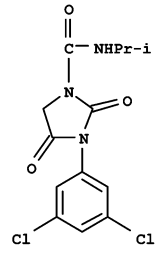	**Amides**	(*44, 45*)

implemented in other cell types (*10*−*12*). Immediately following cell-surface labeling, a tested compound was added to the cell monolayer, and fluorescence signals, induced by membrane interactions of the compound examined, could be monitored spectroscopically or microscopically.

Figure 2 presents the fluorescence dose−response curves recorded for diazinon (*21*), a representative pesticide, following 1.5 h of incubation with the PDA-labeled cells. The concentration-dependent increase in fluorescence signal indicates that binding to and interactions of diazinon with the cell surface indeed were responsible for the chromatic transformations of membrane-incorporated PDA patches. Importantly, the chromatic dose−response curve recorded upon addition of diazinon to the PDA-labeled cells appears different than the respective curve obtained for cell-free vesicles (Supporting Information), most likely reflecting the distinct lipid bilayer environments in artificial lipid/PDA vesicles as compared to the PDA-labeled cells (*10*).

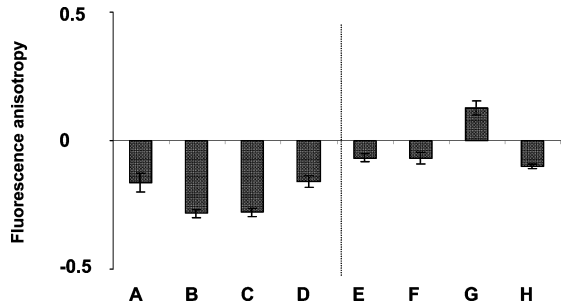

Figure 4. Fluorescence anisotropy of membrane-incorporated TMA-DPH. Net changes recorded after incubation of the A431 cells with (A) allethrin, (B) barban, (C) chlorperifos, (D) diazinon, (E) paraoxon, (F) linuron, (G) cypermethrin, and (H) carbaryl. All compounds were added at 100 μM. The broken line separates the two pesticides groupings; see the text.

Figure 3 presents the time-dependent fluorescence response curves induced within the PDA-labeled cells following incubation with different pesticides (Table 1). The molecules that we examined were widely used in agriculture and were selected from representative pesticide families. Figure 3 demonstrates that significant differences occur in the intensities of fluorescence signals induced by the pesticides tested. Roughly, two groups can be distinguished in Figure 3: compounds that induced a relatively high fluorescence response when incubated with the PDA-labeled cells (diazinon, diuron, chlorperifos, and barban, Figure 3A) and molecules that gave rise to lesser or insignificant fluorescence emission after addition to the chromatic cells (permethrin, cypermethrin, carboxin, paraoxon, allethrin, linuron, pronamide, carbaryl, iprodion, and isoxabene, Figure 3B).

Previous studies have determined that fluorescence emission of membrane-attached PDA is due to binding and perturbations to the lipid bilayer induced by lipophilic molecules interacting with the cell surface, which consequently modulate the conjugated network of the polymer (*10*). Accordingly, the significant differences in the fluorescence responses apparent in Figure 3 are ascribed to the extent of membrane interactions by the tested molecules. Thus, diazinon, diuron, chlorperifos, allethrin, and barban appear highly membrane-active giving rise to high fluorescence from the PDA-labeled cells (Figure 3A). In contrast, the other molecules examined did not disrupt the

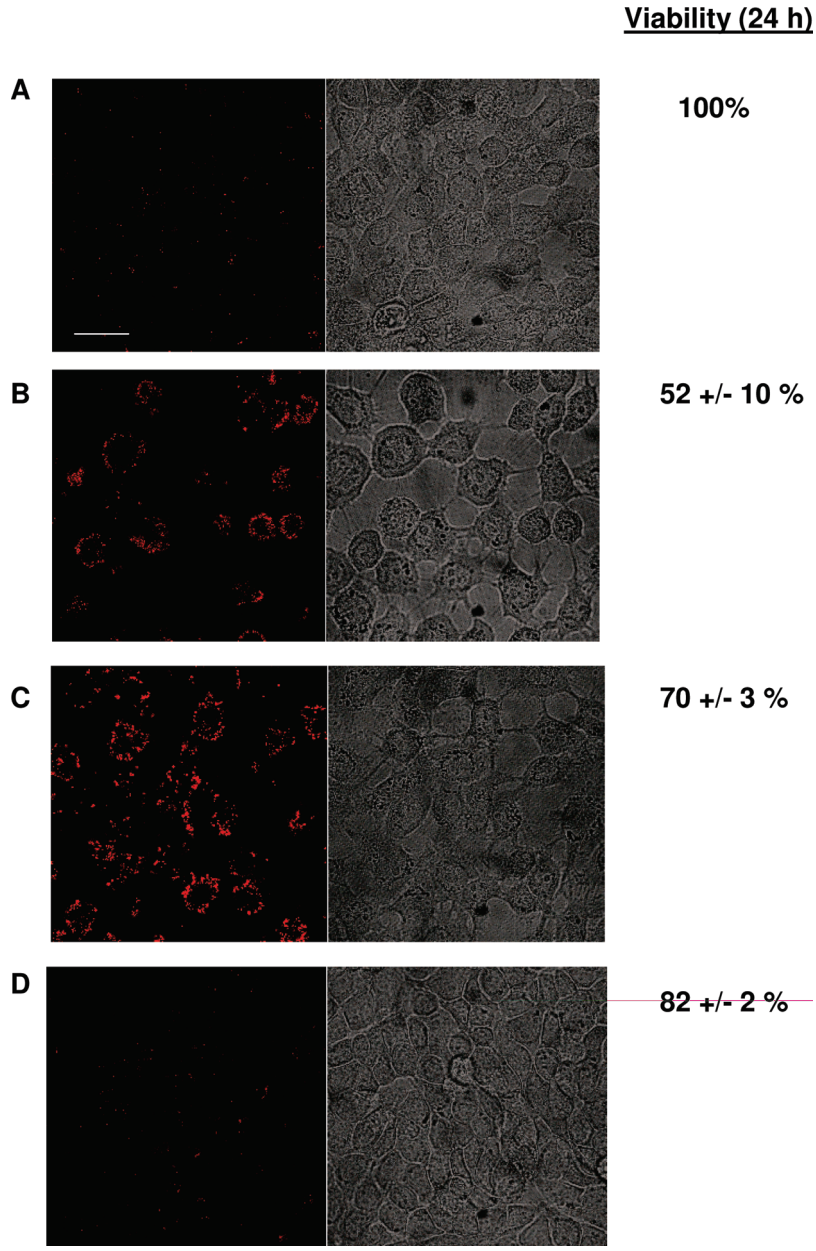

Figure 5. Confocal fluorescence microscopy and viability of PDA-labeled A431 cells. Confocal fluorescent (left) and transmission (right) microscopy images and cell viability determined 24 h after pesticide addition (using CellTiter 96 AQueous One Solution Cell Proliferation assay). All compounds were added at nominal (as-dissolved) concentrations of 500 μM. The viability of the control cells, without pesticide addition, was defined as 100%. (A) Control (no pesticide added), (B) barban added and incubated for 5 min, (C) diazinon added, and (D) linuron added. The scale bar corresponds to 20 μm.

plasma membrane—resulting in negligible fluorescence signals—or exhibited much smaller membrane interactions (Figure 3B).

Another important feature apparent in Figure 3 is the relatively slow increase of the fluorescence signals induced by the membrane-active compounds, reaching plateaus after more than an hour. This result suggests that interactions of the pesticide molecules with the cell membrane are not instantaneous but are rather characterized by slower diffusion/insertion into the lipid bilayer. Time-dependent sigmoid chromatic curves were previously reported for small molecules and peptides undergoing passive diffusion into membrane bilayers (*46*). The slow increase in fluorescence emission is, furthermore, an indication that the fluorescence signal is most likely due to pesticide interactions with the lipid bilayer, rather than nonspecific interactions with the membrane-attached PDA nanopatches (*10*).

To corroborate the proposed relationship between pesticide-induced fluorescence emission in PDA-labeled cells and membrane perturbations, we carried out fluorescence anisotropy experiments utilizing a dye embedded in the cell membrane (Figure 4). The anisotropy measurements were designed to evaluate changes in the fluidity of the membrane bilayer following incubation of the cells with some of the pesticides screened using the PDA-labeled cell assay. In the experiments depicted in Figure 4, we recorded the fluorescence anisotropy of membrane-embedded TMA-DPH, a widely used probe that exhibits significant sensitivity to the dynamics of its lipid bilayer environment (*47*).

The bar diagram in Figure 4 depicts the differences between the final fluorescence anisotropy (after incubation with the tested compounds) and the initial anisotropy of the DPH-incorporated cells. The values shown in Figure 4 indeed mirror the variations in fluorescence response of the PDA-labeled cells induced by

the pesticides (fluorescence curves in Figure 3). In particular, the molecules inducing the greater fluorescence transformations of the PDA-labeled cells (diazinon, allethrin, chlorperifos, and barban) gave rise to experimentally significant negative net anisotropy difference—that is, higher fluidity of the bilayer (Figure 4A−D). On the other hand, lesser membrane-active pesticides according to the PDA fluorescence curves in Figure 3 (cypermethrin, paraoxon, linuron, and carbaryl) produced lesser (or positive) changes in fluorescence anisotropy after incubation with the A431 cells (Figure 4E−H).

Previous reports pointed to fluidity changes in lipid bilayers as a major consequence of binding by membrane-active pharmaceutical molecules, short peptides, and insecticides as well (*3, 48, 49*). Moreover, modification of bilayer ordering and fluidity induced by membrane-active molecules was shown to constitute a primary factor contributing to the chromatic transitions in PDA-labeled cells (*12*). Accordingly, the fluorescence anisotropy data in Figure 4 support the direct relationship between the bilayer perturbation induced by the putative membrane-active pesticides and the fluorescence transformations in the PDA-labeled cells.

While Figure 3 depicts the application of fluorescence spectroscopy for reporting on membrane activity by tested pesticides, fluorescence confocal microscopy can be also used for visualization and rapid analysis of pesticide interactions with the plasma membrane (Figure 5). Figure 5 depicts representative confocal microscopy images of A431 monolayer cells incubated with barban (Figure 5B) and diazinon (Figure 5C), both belonging to the group of putative membrane-active compounds, and linuron (Figure 5D), which was much less membrane-active according to Figures 3 and 4.

Indeed, consistent with the spectroscopy experiments in Figure 3, both barban and diazinon induced dramatic enhancement of the PDA fluorescence (Figure 5B,C). In particular, the vivid visual appearance of abundant fluorescence spots concentrated at the cell borders in Figure 5B,C is a clear consequence of the chromatic transitions of membrane-localized PDA nanopatches. The microscopy image obtained for PDA-labeled cells treated with linuron, on the other hand, is similar to the control cells, that is, yielding only background-level fluorescence (Figure 5D). This microscopy result echoes the minimal membrane activity of linuron, apparent in the data depicted in Figures 3 and 4.

The cell viability values shown in Figure 5 suggest that membrane perturbations indeed lead to increased toxicity. The viability experiments employed a conventional cell proliferation assay (see the Experimental Procedures) to evaluate the percentage of live cells 24 h after incubation with the tested molecules, at the same concentrations employed for the microscopy experiments (note that the viability analysis was carried out for unlabeled cells). The cell viability results indicate that diazinon, for example, which is shown to significantly disrupt the membrane bilayer (Figures 4 and 5), gave rise to almost 50% cell death after 24 h. Barban induced lesser cell death (around 70%, Figure 5C); however, significantly higher viability (around 80%) was recorded for linuron, which exhibited minimal bilayer perturbation according to the confocal fluorescence microscopy experiment (Figure 5D).

Conclusions

This study describes application of a newly developed chromatic live cell assay for evaluating membrane interactions and bilayer perturbations induced by pesticides. The thrust of the chromatic analysis presented here is the hypothesis that pesticide compounds that exhibit significant membrane disruption also display toxic effects; accordingly, the PDA-labeled platform could be a useful vehicle for predicting molecular toxicity based upon the occurrence and extent of plasma membrane interactions. Importantly, the chromatic cell assay cannot eliminate toxicity risks of compounds that are not membrane-active (such molecules could act on intracellular targets); however, the main strength of the new approach is to alert on molecules that do significantly interact with the plasma membrane and thus might exhibit higher probability for adverse physiological effects upon the cell.

The new cell-based assay exhibits two distinct advantages over existing techniques employing small-molecule fluorescence probes (such as DPH, used in this work for corroboration of the chromatic analysis). First, the fluorescence emission of the PDA nanopatches is an "on−off" feature directly related to the occurrence of membrane perturbations within the cell plasma membrane. In particular, because one does not need to analyze relatively small changes in fluorescence anisotropy (in the case of DPH-based dyes, for example), interpretation of data acquired with the PDA-labeled cell platform is more straightforward and unambiguous. Another important feature of the new labeled-cell assay is the possibility for microscopic visualization of membrane perturbations. In contrast to numerous other available fluorescent probes for which fluorescence depends only upon their localization in specific membrane regions or cellular organelles, the PDA fluorescence is directly induced by membrane interactions and perturbations and thus provides an effective probe for localized disruption of the membrane bilayer. Limitations of the new assays should also be highlighted. In particular, lipid bilayer perturbations are not the sole predictor for cellular toxicity; molecules that do not exhibit membrane activity could still induce a variety of toxic effects.

The chromatic assay presented here relies on live cells labeled with chromatic PDA nanopatches that are attached to the plasma membrane. This is a simple, biologically relevant, and versatile platform, amenable to both spectroscopy screening as well as microscopy imaging. Importantly, analysis is conducted in living cells, elucidating processes occurring in the actual cell membrane environment. Furthermore, results are obtained much faster than conventional toxicology screening methods, which are generally technically demanding and take a few days or weeks to perform.

Supporting Information Available: Comparison between chromatic response of lipid/PDA vesicles vs PDA-labeled cells. This material is available free of charge via the Internet at http://pubs.acs.org.

References

(1) Banerjee, B. D., Seth, V., and Ahmed, R. S. (2001) Pesticide-induced oxidative stress: Perspectives and trends. *Rev. Environ. Health 16*, 1–40.
(2) Li, Q., and Kawada, T. (2006) The mechanism of organophosphorus pesticide-induced inhibition of cytolytic activity of killer cells. *Cell. Mol. Immunol. 3*, 171–178.
(3) Antunes-Madeira, M. D. C., Videira, R. A., Lopes, V., and Madeira, V. M. C. (1996) Toxicity of organophosphorus insecticides: Alteration of membrane fluidity. *Med. Sci. Res. 24*, 753–756.
(4) Antunes-Madeira, M. D. C., and Madeira, V. M. C. (1989) Membrane fluidity as affected by the insecticide lindane. *Biochim. Biophys. Acta 982*, 161–166.
(5) Golubev, V. N. (1993) Mechanisms of interaction of pesticides with the lipid bilayer in cell membranes. *Russ. Chem. Rev. 62*, 683–691.
(6) Song, X., Pope, C., Murthy, R., Shaikh, J., Lal, B., and Bressler, J. P. (2004) Interactive effects of paraoxon and pyridostigmine on blood-brain barrier integrity and cholinergic toxicity. *Toxicol. Sci. 78*, 241–247.

(7) Moya-Quiles, M. R., Munoz-Delgado, E., and Vidal, C. J. (1995) Effect of the pyrethroid insecticide allethrin on membrane fluidity. *Biochem. Mol. Biol. Int. 36*, 1299–1308.
(8) Videira, R. A., Peca, L. P. S., Antunes-Madeira, M. D. C., and Madeira, V. M. C. (1994) Effects of malathion on membrane fluidity and its implications for the mechanisms of toxicity. *Med. Sci. Res. 22*, 551–553.
(9) Suwalsky, M., Benites, M., Norris, B., and Sotomayor, C. P. (2003) The organophosphorous insecticide chlorpyrifos affects the neuroepithelial junction, the bioelectric parameters of the skin of the frog Caudiverbera caudiverbera, and the structure of model cell membranes. *Pestic. Biochem. Physiol. 77*, 44–53.
(10) Orynbayeva, Z., Kolusheva, S., Livneh, E., Lichtenshtein, A., Nathan, I., and Jelinek, R. (2005) Visualization of membrane processes in living cells by surface-attached chromatic polymer patches. *Angew. Chem., Int. Ed. Engl. 44*, 1092–1096.
(11) Orynbayeva, Z., Kolusheva, S., Groysman, N., Gavrielov, N., Lobel, L., and Jelinek, R. (2007) Vaccinia virus interactions with the cell membrane studied by new chromatic vesicle and cell sensor assays. *J. Virol. 81*, 1140–1147.
(12) Groysman, N., Orynbayeva, Z., Katz, M., Kolusheva, S., Khanin, M., Danilenko, M., and Jelinek, R. (2008) Membrane processes and biophysical characterization of living cells decorated with chromatic polydiacetylene vesicles. *Biochim. Biophys. Acta 1778*, 1335–1343.
(13) Kolusheva, S., Wachtel, E., and Jelinek, R. (2003) Biomimetic lipid/polymer colorimetric membranes: molecular and cooperative properties. *J. Lipid Res. 44*, 65–71.
(14) Ma, G., and Cheng, Q. (2005) A vesicular polydiacetylene sensor for colorimetric signaling of bacterial pore-forming toxin. *Langmuir 21*, 6123–6126.
(15) Okada, S. Y., Jelinek, R., and Charych, D. H. (1999) Induced color change of conjugated polymeric vesicles by interfacial catalysis of phospholipase A2. *Angew. Chem., Int. Ed. Engl. 38*, 655–659.
(16) Pevzner, A., Kolusheva, S., Orynbayeva, Z., and Jelinek, R. (2008) Giant chromatic lipid/polydiacetylene vesicles for detection and visualization of membrane interactions. *Adv. Funct. Mater. 18*, 242–247.
(17) Errien, N., Mevellec, J.-Y., Louarn, G., and Froyer, G. (2005) Polymerization of diacetylene-bis(toluenesulfonide) in a porous silica matrix: Evidence of polymer chain self-orientation. *Chem. Mater. 17*, 2803–2806.
(18) Volinsky, R., Kliger, M., Sheynis, T., Kolusheva, S., and Jelinek, R. (2007) Glass-supported lipid/polydiacetylene films for colour sensing of membrane-active compounds. *Biosens. Bioelectron. 22*, 3247–3251.
(19) Epand, R. F., Schmitt, M. A., Gellman, S. H., Sen, A., Auger, M., Hughes, D. W., and Epand, R. M. (2005) Bacterial species selective toxicity of two isomeric alpha/beta-peptides: role of membrane lipids. *Mol. Membr. Biol. 22*, 457–469.
(20) Cory, A. H., Owen, T. C., Barltrop, J. A., and Cory, J. G. (1991) Use of an aqueous soluble tetrazolium/formazan assay for cell growth assays in culture. *Cancer Commun. 3*, 207–212.
(21) Jameson, R. R., Seidler, F. J., and Slotkin, T. A. (2007) Nonenzymatic functions of acetylcholinesterase splice variants in the developmental neurotoxicity of organophosphates: Chlorpyrifos, chlorpyrifos oxon, and diazinon. *Environ. Health Perspect. 115*, 65–70.
(22) Mankame, T., Hokanson, R., Fudge, R., Chowdhary, R., and Busbee, D. (2006) Alteration of gene expression in human cells treated with the agricultural chemical diazinon: Possible interactions in fetal development. *Hum. Exp. Toxicol. 25*, 225–233.
(23) Flaskos, J., Harris, W., Sachana, M., Muñoz, D., Tack, J., and Hargreaves, A. J. (2007) The effects of diazinon and cypermethrin on the differentiation of neuronal and glial cell lines. *Toxicol. Appl. Pharmacol. 219*, 172–180.
(24) Qiao, D., Seidler, F. J., and Slotkin, T. A. (2005) Oxidative mechanisms contributing to the developmental neurotoxicity of nicotine and chlorpyrifos. *Toxicol. Appl. Pharmacol. 206*, 17–26.
(25) Kousba, A. A., Sultatos, L. G., Poet, T. S., and Timchalk, C. (2004) Comparison of chlorpyrifos-oxon and paraoxon acetylcholinesterase inhibition dynamics: Potential role of a peripheral binding site. *Toxicol. Sci. 80*, 239–248.
(26) Tuler, S. M., and Bowen, J. M. (1989) Toxic effects of organophosphates on nerve cell growth and ultrastructure in culture. *J. Toxicol. Environ. Health 27*, 209–223.
(27) Hildebrand, M. E., McRory, J. E., Snutch, T. P., and Stea, A. (2004) Mammalian voltage-gated calcium channels are potently blocked by the pyrethroid insecticide Allethrin. *J. Pharmacol. Exp. Ther. 308*, 805–813.
(28) Ginsburg, K., and Narahashi, T. (1999) Time course and temperature dependence of allethrin modulation of sodium channels in rat dorsal root ganglion cells. *Brain Res. 847*, 38–49.
(29) Nishimura, M., Obana, N., Yagasaki, O., and Yanagiya, I. (1984) Involvement of adrenergic and serotonergic nervous mechanisms in allethrin-induced tremors in mice. *J. Toxicol. Sci. 9*, 131–142.
(30) Rosita, G., Giancarlo, F., and Cinzia, N. (2002) Cypermethrin-induced plasma membrane perturbation on erythrocytes from rats: reduction of fluidity in the hydrophobic core and in glutathione peroxidase activity. *Toxicology 175*, 91–101.
(31) Paul, E. A., Simonin, H. A., and Tomajer, T. M. (2005) A Comparison of the toxicity of synergized and technical formulations of permethrin, sumithrin, and resmethrin to trout. *Arch. Environ. Contam. Toxicol. 48*, 251–259.
(32) Singh, A., and Srivastava, V. K. (1999) Toxic effect of synthetic pyrethroid permethrin on the enzyme system of the freshwater fish Channa striatus. *Chemosphere 39*, 1951–1956.
(33) Tenreiro, S., Vargas, R. C., Teixeira, M. C., Magnani, C., and Sa-Correia, I. (2005) The yeast multidrug transporter Qdr3 (Ybr043c): Localization and role as a determinant of resistance to quinidine, barban, cisplatin, and bleomycin. *Biochem. Biophys. Res. Commun. 327*, 952–959.
(34) Hoffman, J. C. (1995) N-Phenylcarbamate mitotic disrupter herbicides vary in ability to induce cytoskeletotoxicity in human cells. *In Vitro Toxicol. 8*, 277–282.
(35) Moreno, A. J. M., Serafim, T. I., and Madeira, P. J. O. (2007) Inhibition of mitochondrial bioenergetics by carbaryl is only evident for higher concentrations—Relevance for carbaryl toxicity mechanisms. *Chemosphere 66*, 404–411.
(36) Mahajan, R., Blair, A., Coble, J., Lynch, C. F., Hoppin, J. A., Sandler, D. P., and Alavanja, M. C. R. (2007) Carbaryl exposure and incident cancer in the Agricultural Health Study. *Int. J. Cancer 121*, 1799–1805.
(37) Nandan, D., and Wagle, D. S. (1980) Metabolic effect of carboxin in rat. *Prog. Ecol. 5/7*, 305–312.
(38) DellaGreca, M., Lesce, M. R., Cermola, F., Rubino, M., and Isidori, M. (2004) Phototransformation of carboxin in water. Toxicity of the pesticide and its sulfoxide to aquatic organisms. *J. Agric. Food Chem. 52*, 6228–6232.
(39) Mazzolenica, G., Telo, P., Camplani, A., Tanganelli, S., Monarca, S., and Ragnotti, G. (1994) Influence of the herbicide Linuron on growth rate and gap-junctional intercellular communication of cultured endothelial cells. *J. Environ. Pathol. Toxicol. Oncol. 13*, 1–10.
(40) Erkell, L. J., and Walum, E. (1979) Differentiation of cultured neuroblastoma cells by urea derivatives. *FEBS Lett. 104*, 401–404.
(41) Vinggaard, A. M., Breinholt, V., and Larsen, J. C. (1999) Screening of selected pesticides for oestrogen receptor activation in vitro. *Food Addit. Contam. 16*, 533–542.
(42) Huang, X., Fong, S., Deanovic, L., and Young, T. M. (2005) Toxicity of herbicides in highway runoff. *Environ. Toxicol. Chem. 24*, 2336–2340.
(43) Reuber, M. D. (1980) Carcinogenicity of pronamide. *Environ. Res. 23*, 1–12.
(44) Ghisari, M., and Bonefeld-Jorgensen, E. C. (2005) Impact of environmental chemicals on the thyroid hormone function in pituitary rat GH3 cells. *Mol. Cell. Endocrinol. 244*, 31–41.
(45) Andersen, H. R., Vinggaard, A. M., Rasmussen, T. H., Gjermandsen, I. M., and Bonefeld-Jorgensen, E. C. (2002) Effects of currently used pesticides in assays for estrogenicity, androgenicity, and aromatase activity in vitro. *Toxicol. Appl. Pharmacol. 179*, 1–12.
(46) Jelinek, R., and Kolusheva, S. (2001) Polymerized lipid vesicles as colorimetric biosensors for biotechnologycal applications. *Biotechnol. Adv. 19*, 109–118.
(47) Illinger, D., Duportail, G., Mely, Y., Poirel-Morales, N., Gerard, D., and Kuhry, J. G. (1995) A comparison of the fluorescence properties of TMA-DPH as a probe for plasma membrane and for endocytic membrane. *Biochim. Biophys. Acta 1239*, 58–66.
(48) Andersson, A., Biverstahl, H., Nordin, J., Danielsson, J., Lindahl, E., and Maeler, L. (2007) The membrane-induced structure of melittin is correlated with the fluidity of the lipids. *Biochim. Biophys. Acta, Biomembr. 1768*, 151–121.
(49) Tangorra, A., Curatola, G., and Bertoli, E. (1991) Evaluation of antiepileptic drug effect on membrane fluidity. *Exp. Mol. Pathol. 55*, 180–189.

TX800206T